Earthquakes and Structures, *Vol. 6, No. 3 (2014) 317-334*
DOI: http://dx.doi.org/10.12989/eas.2014.6.3.317

Monotonic and cyclic flexural tests on lightweight aggregate concrete beams

E.G. Badogiannis and M.D. Kotsovos*

Civil Engineering Department, National Technical University of Athens, Athens 15773, Greece

(Received July 3, 2013, Revised November 22, 2013, Accepted December 9, 2013)

Abstract. The work is concerned with an investigation of the advantages stemming from the use of lightweight aggregate concrete in earthquake-resistant reinforced concrete construction. As the aseismic clauses of current codes make no reference to lightweight aggregate concrete beams made of lightweight aggregate concrete but designed in accordance with the code specifications for normal weight aggregate concrete, together with beams made from the latter material, are tested under load mimicking seismic action. The results obtained show that beam behaviour is essentially independent of the design method adopted, with the use of lightweight aggregate concrete being found to slightly improve the post-peak structural behaviour. When considering the significant reduction in deadweight resulting from the use of lightweight aggregate concrete, the results demonstrate that the use of this material will lead to significant savings without compromising the structural performance requirements of current codes.

Keywords: beams; earthquake-resistant design; lightweight aggregate concrete; cyclic tests

1. Introduction

Lightweight aggregate concrete (LWAC) is made through the use of lightweight aggregates which can be either of natural origin, such as pumice and scoria, or made from industrial by-products, such as the fly ash aggregates (Short and Kinniburg 1978, Gunduz 2008, Swamy and Lambert 1984). Pumice is a pyroclastic rock which has been used throughout the world for centuries, as it can be found in many places where volcanic eruptions occur. It originates from acidic lavas, has a very low density and often floats in the water. Mixing pumice aggregates with Portland cement and water produces a fire-resistant LWAC with excellent sound and thermal insulation properties, useful in a wide range of applications in the construction industry (Gunduz 2008).

Moreover, it is widely recognised that, under normal loading conditions, the use of lightweight-aggregate concrete (LWAC) in reinforced-concrete (RC) construction often offers significant advantages over the use of normal-weight aggregate concrete (NC). A notable case of the application of LWAC in RC construction is the cantilever roof of the Twickenham Grandstand built by I. Bobrowski & Partners (Clarke 1993). And yet, in spite of the large amount research work carried out under monotonic loading (e.g. Ahmad and Barker 1991, Ahmad and Batts 1991,

*Corresponding author, Ph. D., E-mail: mkotsov@central.ntua.gr

http://www.techno-press.org/?journal=eas&subpage=7 ISSN: 2092-7614 (Print), 2092-7622 (Online)

Hanson 1957, Hognestad *et al.*. 1964, Ivey and Buth 1967, Kang *et al.*. 2011, Kong *et al.*. 1996, Kripanarayanan and Branson 1972, Salamandra and Ahmad 1990, Schaumann *et al.*. 2009, Yang 2010, Yang *et al.*. 2013), the use of LWAC in construction is rather limited, since its production requires additional skills and more technology back up than NC and there is a feeling of uncertainty regarding its structural performance, even though current codes for the structural use of concrete under normal conditions, such as, for example, ACI 318 (American Concrete Institute 2011) and EC2 (Eurocode 2 2004), include provisions for the design of RC structures made of LWAC. In fact, this rather limited use of LWAC in RC construction under normal conditions, when compared with the wide use of NC, appears to have discouraged the structural assessment of RC members made of LWAC and designed so as to be earthquake-resistant, since experimental work carried out to date on the seismic behaviour of LWAC members is rather sparse (Kripanarayanan and Branson 1972, Bertero *et al.*. 1980, Ghosh *et al.*. 1993, Rabbat *et al.*. 1986, Kowalski *et al.*. 1999, Marsout *et al.*. 2001, Campione *et al.*. 2005, Chai and Anderson 2005, Mitchell and Marzouk 2007, Hendrix and Kowalsky 2010). As a result, the relevant current codes, such as, for example, ACI 318 (American Concrete Institute 2011) and EC8 (Eurocode 8 2004), hardly make any reference to the use of LWAC in their provisions for the aseismic design of RC structures.

On the other hand, energy conservation is an important issue of any national energy strategy, and significant effort is directed towards improving the thermal insulation of buildings through the use of LWAC (Hassan 1999). Concrete is a key material in avoiding heat losses in buildings and, as the aggregate content of concrete is nearly 80%, the use of lightweight aggregates instead of normal-weight aggregates, leads to considerable improvement of the thermal insulation of concrete buildings (Neville 1999, Khan 2992, Demirboga 2007). Thus, the use of LWAC as a structural building material appears to need reexamination and research on the material’s structural performance is deemed to be more urgent than ever (Short and Kinniburg 1978).

To this end, the present work is intended to provide experimental information on the earthquake-resistant capabilities of RC beams made of LWAC. It is based on a comparative study of the results obtained from tests in which specimens made of LWAC and NC are subjected to cyclic statically applied loading. All specimens are designed in compliance with the provisions of current codes for earthquake-resistant RC structures made from NC. The LWAC selected for the specimens is designed so as to have a uniaxial cylinder compressive strength similar to that of the NC used in spite of being lighter by about 30%.

2. Experimental programme

2.1 Design details

The beams investigated are designated by using a three part name, the first part indicating the type of concrete used (NC for normal concrete and LWAC for lightweight aggregate concrete), the second part, the cross section shape (R for a rectangular and S for a square cross section) and the third part, the type of loading (C for cyclic and M for monotonic) followed by the beam number (1 or 2) when more than one specimens are tested for a particular type of loading.

The total number of beams tested is nine; their design details are shown in Fig. 1. From the figure, it can be seen that all beams have a length l = 2300 mm and a clear span of 1950 mm; those with a rectangular cross section have 150 mm width and 300 mm height, whereas those with a square cross section have a 200 mm side. All beams are reinforced with three 16 mm diameter

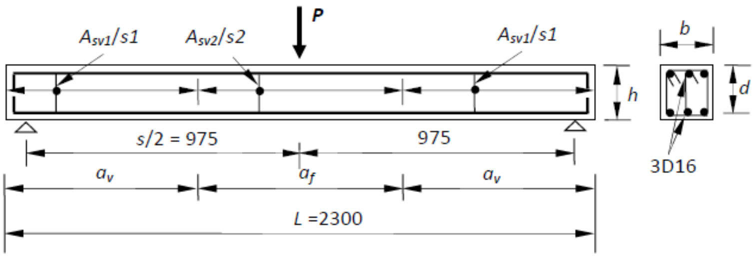

Specimens	b	h	d	a_v	a_f	$A_{sv1}/s1$	$A_{sv2}/s2$
NC-S-C	200	200	170	750	800	D8@160	D8@50
NC-R-C	150	300	270	750	800	D8@150	D8@50
NC-R-M	150	300	270	750	800	D8@150	D8@50
LWAC-S-C	200	200	170	850	600	D8@125	D8@50
LWAC-R-C	150	300	270	750	800	D8@150	D8@50

For beams LWAC-R-M, bottom reinforcement also comprises 3D16, whereas the top longitudinal reinforcement comprises 2D14 rather than 3D16 and the transverse reinforcement two-, rather than three-, legged stirrups

All dimensions in mm

Fig. 1 Design details of specimens tested

longitudinal tension bars, and, with the exception of beams LWAC-R-M, with three 16 mm diameter longitudinal compression bars; the yield stress/strength of the 16 mm diameter bars is 560/620 MPa. In beams LWAC-R-M, the latter bars are replaced with two 14 mm longitudinal bars with a yield stress/strength of 610/670 MPa. The distance of all bars' axes from the top or bottom beam faces is 30 mm. Transverse reinforcement comprises 8 mm diameter two legged, for beams LWAC-R-M, and three legged, in all other cases, stirrups with a yield stress of 550 MPa.

The LWAC mix was designed in accordance with ACI211.2 (American Concrete Institute 1998) and its details are presented in Table 1. The uniaxial cylinder compressive strength f_c and

Table 1 Mix details of LWAC

Ingredients	Cement – CEM II-M(P-LL) 42.5N	Pumice (0-8 mm)	Total water*	Super-plastisizer – CHEM174, Domulco	Effective W/C
kg/m^3	350	1010	300	4	0.42

**depending on absorption capacity of pumice aggregate*

Table 2 Strength, strain at strength and density of LWAC and stress-strain characteristics of each of the beams tested

Beam	LWAC -R-M	LWAC -S-M	LWAC -R-C1	LWAC -R-C2	LWAC -S-C1	LWAC -S-C2
f_c (Mpa)	36.40	32.40	26.50	22.80	25.20	28.00
ε_cx10^3	2.3	2.4	2.2	2.2	2.1	2.2
Density (Kg/m^3)	1640	1630	1560	1460	1480	1460

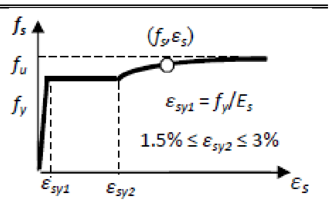

Steel σ-ε curve

Table 3 Mix details of NC

Ingredients	Cement – CEM II-M(P-LL) 42.5N	Fine aggregate (0 - 4 mm)	Coarse aggregate (2-8 mm)	Coarse aggregate (4-16 mm)	Effective W/C
kg/m3	300	920	550	370	0.52

corresponding strain ε_c at the time of testing (at about 2 months after casting) together with the unit weight of the concrete for each of the LWAC beam tested are given in Table 2; the table also includes the stress-strain characteristics of the steel reinforcement used. The cylinder strength and corresponding strain of NC at the time of testing of the specimens is f_c = 34 MPa and $\varepsilon_c \approx 2\text{x}10^{-3}$, respectively, at an age of around 2 months, whereas its mix details are shown in Table 3.

2.2 Loading regimes

The beams are subjected to two types of loading, monotonic and cyclic. In both cases, load is applied in the form of statically increasing displacements imposed at mid span. In the case of monotonic loading, the displacement increases to failure, whereas in the case of cyclic loading, it varies between predefined values which progressively increase to failure. For both types of loading, failure is considered to occur when the sustained load becomes smaller than 85% the peak load value. Three load cycles are carried out for each of the above predefined values with a displacement rate of 0.25 mm/s.

The load is applied through steel plates which are in contact either with the top and bottom faces of the beam as indicated in Fig. 2 or with the end faces of concrete stubs monolithically connected to the beams as indicated in Figs. 6 and 8. The latter method of application has been adopted elsewhere (Kotsovos *et al.* 2013) in order to demonstrate that the results obtained are similar to those obtained through the use of the former method of load application (Kotsovos 2011).

2.3 Experimental set-up

The experimental arrangement used for the tests comprises two identical steel portal frames, with a double-T cross-section, bolted in parallel onto the laboratory strong floor at a distance equal to the specimen’s span. As shown in Fig. 2, the specimens are supported on roller supports positioned underneath the bottom flange of the frame beams so that the reactions can act either upwards or downwards depending on the sense of the transverse displacement. The transverse displacement is applied at the specimens’ mid span through a double-stroke 500 kN hydraulic actuator fixed to the laboratory strong floor. It is interrupted at regular intervals, corresponding to displacement increments of approximately 5 mm, during which the load is maintained constant for at least 1 min in order to mark cracks and take photographs of the specimen’s crack pattern. The load is measured by using a load cell, while the deformation response is measured by linear voltage differential transducers (LVDTs) measuring the specimen deflection at the location of the transverse load point. The forces and displacements are recorded by using a computer-based data-acquisition system.

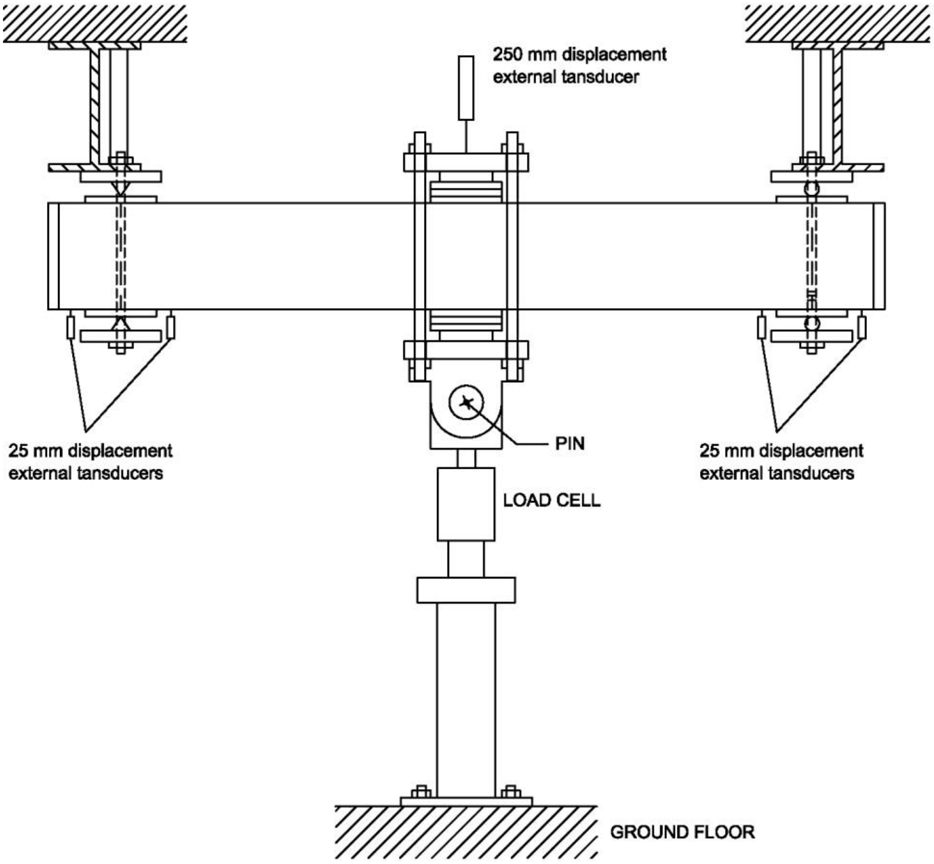

Fig. 2 Experimental set-up

2.4 Design

All beams are designed by implementing the code provisions for structural elements made from normal weight concrete. They are designed so that their load-carrying capacity is reached when their base cross-section attains its flexural capacity, the latter condition being referred to henceforth as *plastic-hinge* formation. Using the cross-sectional and material characteristics of the beams and the EC2 recommended rectangular stress block, the flexural capacity M_f of the elements is calculated from first principles and setting all material safety factors equal to 1. Using M_f, the wall load-carrying capacity P_f (and, hence, the corresponding shear force $V_f = P_f/2$) is easily calculated from static equilibrium. The values of M_f and P_f for each of the specimens tested are given in Table 4 together with the experimentally-established values of the load-carrying capacity (P_e). The table also includes the values of bending moment M_y and load P_y which correspond at the yielding of the beam cross section considered to occur when either the tensile flexural steel yields or concrete strain at the extreme compressive fibre reaches the value of 0.002; the values of P_y are used for assessing the ductility factors of the specimens tested.

The transverse reinforcement (stirrups) of the specimens is designed in compliance with the earthquake-resistant design clauses of EC2 and EC8. The stirrup arrangement of the specimens

Table 4 Calculated values of bending moment M_y and corresponding force P_y at yield, flexural capacity M_f and corresponding load-carrying capacity P_f and experimentally-established values of load-carrying capacity P_e

Specimens	M_y (kNm)	P_y (kN)	M_f (kNm)	P_f (kN)	P_e (kN)	P_e/P_f
NC-R-M	79	162	81	167	177	1.06
NC-R-C	79	162	81	167	172	1.03
NC-S-C	48	98	49	106	112	1.06
LWAC-R-M1	80	173	87	189	206	1.09
LWAC-R-M2	79	172	87	188	207	1.1
LWAC-R-C1	80	173	82	180	185	1.03
LWAC-R-C2	80	173	82	177	184	1.04
LWAC-S-C1	46	100	49	106	109	1.03
LWAC-S-C2	49	105	49	107	109	1.02

tested is shown in Fig. 1. From the figure, it is interesting to note the densely spaced stirrups (designated as A_{sv2}) within the "critical regions" (designated as a_f) specified by the Codes in order to provide confinement to concrete. Such spacing results from expression 5-13 in EC8 (clause 5.4.3.1.2). On the other hand, the stirrups in the remainder of the beams (designated as a_v in Fig. 1), designed in compliance with the code requirements (see clauses 6.2 and 9.6 in EC2), is considered to improve the beams' shear capacity so as to prevent shear failure occurring before flexural capacity is exhausted.

3. Results of tests

The main results of the work are given in Figs. 3 to 22 and Tables 4 and 5. Figs. 3, 5, 7, 9, 11, 13, 15, 17, and 19 show the curves describing the relationship between load and imposed

Table 5 Displacements $\delta_{y,n}$, δ_{sust}, δ_{fail} corresponding at nominal yield, sustained load cycle, and load cycle at failure, respectively, together with the values of the ductility ratio at the sustained load cycle (μ_{sust}) and the load cycle at failure (μ_{fail})

Specimens	δ_{yn} (mm)	δ_{sust} (mm)	δ_{fail} (mm)	μ_{sust}	μ_{fail}
NC-R-M	7	59.5	-	8.5	-
NC-R-C	8.9	26.7	37.8	3	4.2
NC-S-C	9.9	26.6	33.6	2.7	3.14
LWAC-R-M1	11.2	120	-	10.7	-
LWAC-R-M2	9,4	105	-	10.6	-
LWAC-R-C1	8.8	28.2	39.5	3.2	4.5
LWAC-R-C2	8,6	25.1	29.2	2.92	3.4
LWAC-S-C1	13.3	53.1	63.1	4	3.4
LWAC-S-C2	13.8	50.3	67.5	3.64	4.8

displacement of the specimens tested. For purposes of comparison, the curves are presented in a normalised form, the load being normalised with respect to the value of the peak load, whereas the displacement with respect to the nominal displacement at yield (calculated as described later).

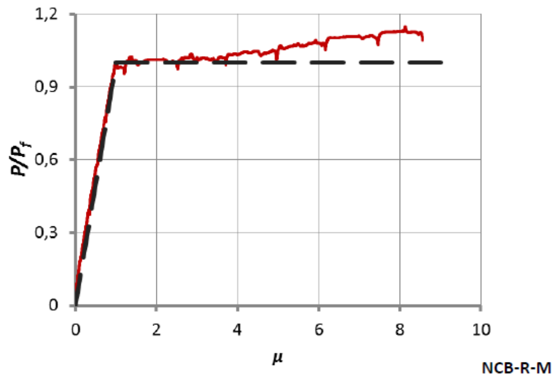

Fig. 3 Load-deflection curve of beam NCB-R-M under monotonic loading with intersection of dash lines indicating 'nominal yield'

Fig. 4 Failure mode of beam NCB-R-M under monotonic loading

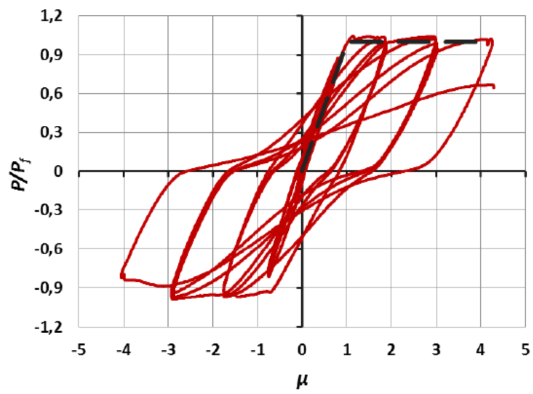

Fig. 5 Load-deflection curve of beam NCB-R-C under cyclic loading with intersection of dash lines indicating 'nominal yield'

Fig. 6 Failure mode of beam NCB-R-C under cyclic loading

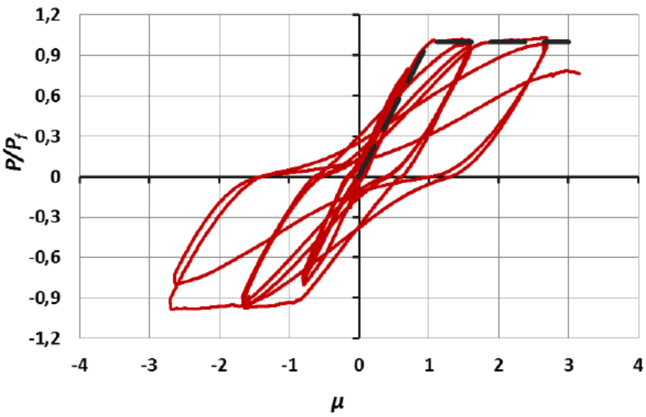

Fig. 7 Load-deflection curve of beam NCB-S-C under cyclic loading with intersection of dash lines indicating ‘nominal yield’

Fig. 8 Failure mode of beam NCB-S-C under cyclic loading

Figs. 4, 6, 8, 10, 12, 14, 16, 18 and 20 depict the specimens’ crack pattern at failure, whereas Figs. 21 and 22 show the variation of the energy dissipated during successive load cycles. The dissipated

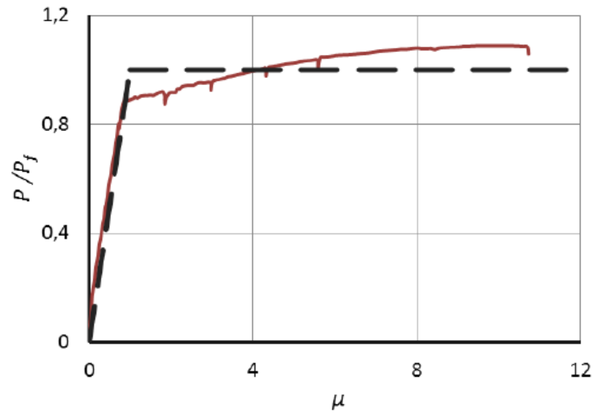

Fig. 9 Load-deflection curve of beam LWAC-R-M1 under monotonic loading with intersection of dash lines indicating 'nominal yield'

LWAC-R-M1

Fig. 10 Failure mode of beam LWAC-R-M1 under monotonic loading

energy during each cycle is expressed in a form normalized with respect to a nominal value of the elastic energy expressed as $E_y = 0.5 \cdot P_y \cdot \delta_y$.

Table 4 shows the calculated values of the bending moment and corresponding load at yield, together with those of the flexural and load-carrying capacities of the beams investigated; the table also includes the values of the experimentally established peak load sustained by the specimens. Finally, Table 5 provides the values of the nominal displacement at yield, of the maximum sustained displacement and of the displacement at failure together with the corresponding values of the ductility ratio defined as the ratio of the maximum sustained displacement or displacement at failure to the nominal displacement at yield. The latter is determined in the manner described below:

(a) The cross section's bending moment at yield, M_y (assessed by assuming that yielding occurs when either the concrete strain at the extreme compressive fibre attains a value of 0.002 or the tension reinforcement yields), and flexural capacity, M_f, are first calculated.

(b) By using the values of M_y and M_f derived in (a), the corresponding values of the transverse load at yield, P_y, and at flexural capacity, P_f, are obtained from the equilibrium equations $P_y = M_y/a_{ss}$ and $P_f = M_f/a_{ss}$, where a_{ss} is the beam shear span. (Note that a_{ss} is obtained by subtracting half the loading- plate length from half the beam span *s*.)

In the figures describing the load-displacement curves, a line is drawn through the points of the load-displacement curves at P=0 and P=P_y. This line is extended to the load level P_f. The displacement $\delta_{y,n}$ corresponding to P_f is used to calculate the values of the ductility ratios $\mu_{sust} = \delta_{sust}/\delta_{y,n}$ and $\mu_{fail} = \delta_{fail}/\delta_{y,n}$ included in Table 5.

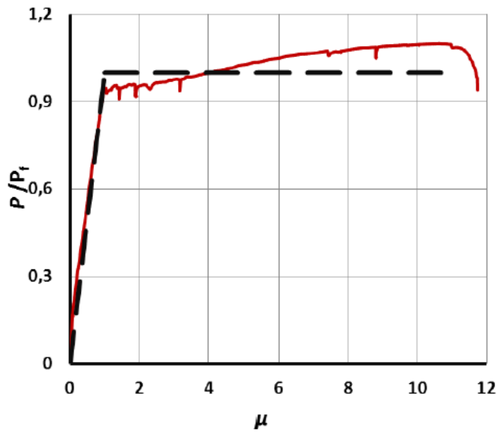

Fig. 11 Load-deflection curve of beam LWAC-R-M2 under monotonic loading with intersection of dash lines indicating 'nominal yield'

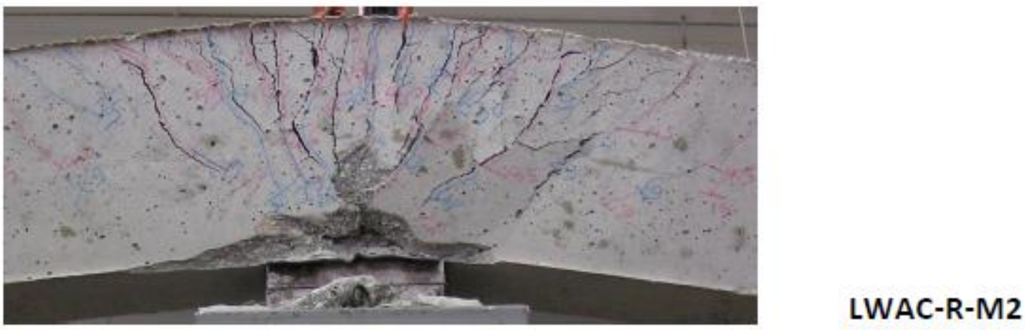

Fig. 12 Failure mode of beam LWAC-R-M2 under monotonic loading

4. Discussion of results

From Table 4, it can be seen that beams LWAC-R-C1 and LWAC-R-C2 and beams LWAC-S-C1 and LWAC-S-C2, which are essentially replicas, are characterised by load-carrying capacities exhibiting a small, if any deviation, in spite of the differences in strength of the LWAC used for each of the replica beams tested. Moreover, from Table 4, it can be seen that the replica beams are also characterised by a small deviation of the values of nominal displacement at yield. It appears from the above, therefore, that the results obtained from the tests on the beams made from lightweight aggregate concrete (LWAC) are as reproducible as those obtained from tests on normal weight aggregate concrete (NC) and, hence, one test is sufficient for establishing a structural member’s behaviour.

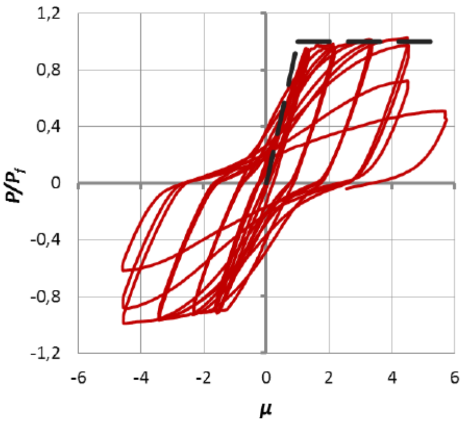

Fig. 13 Load-deflection curve of beam LWAC-R-C1 under cyclic loading with intersection of dash lines indicating ‘nominal yield’

Fig. 14 Failure mode of beam LWAC-R-C1 under cyclic loading

From the last column of Table 4, it is clearly seen that, for all specimens, the calculated values of load-carrying capacity underestimate their experimentally established counterparts by an amount which varies between approximately 2% and 10%. This underestimate appears to be slightly larger when the specimens are tested under monotonic loading, particularly in the case of specimens made of LWAC. As regards the values of load-carrying capacity obtained from tests on beams under cyclic loading, the deviation of the calculated values from their experimental counterparts appears to be independent of the type of concrete used to manufacture the specimens.

From Tables 4 and 5, it is noted that the load-carrying capacity (P_e) of the beams tested is independent of the type of concrete used and the loading regime adopted. However, as regards the nominal displacement at yield (δ_{ny}), this is found to be independent of the type of concrete used only for the specimens with a rectangular cross section (compare specimen NC-R-C with specimens LWAC-R-C1 and LWAC-R-C2) when subjected to cyclic loading; in all other cases, δ_{ny}

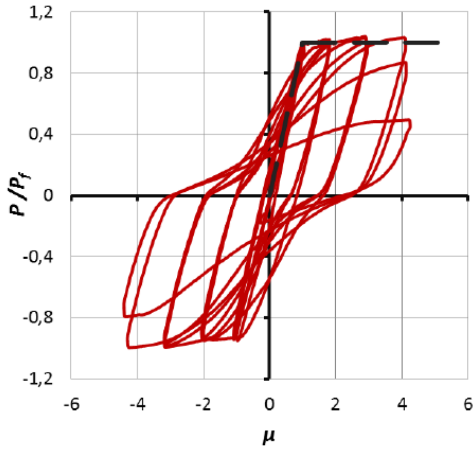

Fig. 15 Load-deflection curve of beam LWAC-R-C2 under cyclic loading with intersection of dash lines indicating ‘nominal yield’

Fig. 16 Failure mode of beam LWAC-R-C2 under cyclic loading

of the beams made of NC is smaller than its counterpart for the LWAC beams by about 30%. Although such behaviour may be partly attributed to increased deformability of LWAC due to the larger porosity of the lightweight aggregates, the method of assessment of δ_{ny} combined with the scatter of the experimental results may also contribute significantly. Since the ratio P_e/δ_{ny} provides an indication of the beams’ stiffness, it appears that, while the load-carrying capacity of the beams under both monotonic and cyclic loading is essentially independent of the types of concrete used in the present work, the beams made of LWAC are more deformable than their counterparts made of NC.

Monotonic loading - *As* indicated in Figs. 3, 9 and 11 and Table 4 and 5, the beams exhibit similar trends of behaviour under monotonic loading, in spite of the differences in the type of concrete used. However, the ductility ratio at the peak load level of the beams made of LWAC (see Figs. 9 and 11) is larger by about 25% than its counterpart of the beam made from NC. On the other hand, all beams exhibit similar crack patterns with increasing load and a similar mode of failure in that the loss of load-carrying capacity is preceded by failure of the compressive zone at their mid cross section (see Figs. 4, 10 and 12). The above findings are in agreement with those

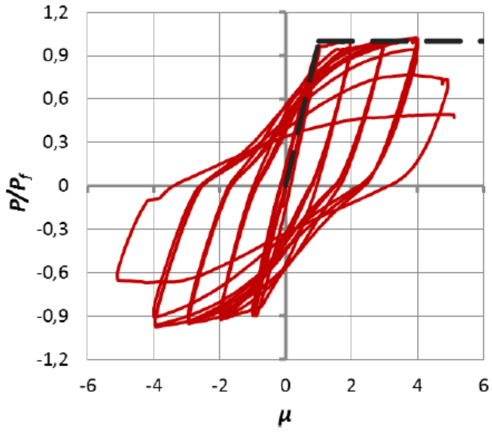

Fig. 17 Load-deflection curve of beam LWAC-S-C1 under cyclic loading with intersection of dash lines indicating 'nominal yield'

Fig. 18 Failure mode of beam LWAC-S-C1 under cyclic loading

already reported (e.g., Sin *et al.* 2011).

Cyclic loading - From in Figs. 5, 13 and 15, comparing the load-displacement curves of the beams with the rectangular cross section, shows that beams NC-R-C and LWAC-R-C1/C2 exhibit similar behaviour, in spite of the difference in the type of the concrete material used to construct the specimens. On the other hand, for the beams with a square cross section, comparing the load-displacement curves shown in Figs. 7, 17, and 19 indicates that the beams made of LWAC (beams LWAC-S-C1/C2) exhibit better post peak behaviour than their counterpart made of NC (beam NC-S-C) in that they sustain three additional load cycles to a ductility ratio larger than 3.5 as compared with the ductility ratio of 2.7 sustained by beam NC-S-C. In all cases, however, the achieved ductility ratio is larger than the code demand of 1.5 for medium (DCM) and 2.0 for high (DCH) ductility (see Table 5.1 in EC8 for inverted pendulum systems). Such behaviour is in agreement with that reported in Rabbat *et al.* (1986) for the case of NC and LWAC columns under cyclic loading; in fact, this similarity in NC and LWAC structural response led Rabbat *et al.* (1986) to conclude that the ACI requirements for column confinement for NC columns can be extended to cover the case LWAC columns. It should be noted, however, that, although as regards the displacement capacity of NC and LWAC columns, the test results by Rabbat *et al.* (1986) are in agreement with those obtained by Kowalski *et al.* (1999), the latter report a reduced contribution

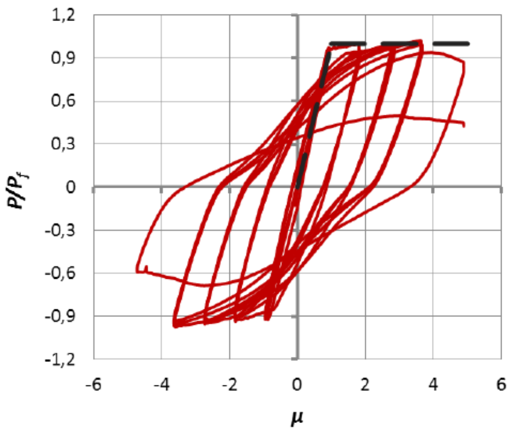

Fig. 19 Load-deflection curve of beam LWAC-S-C2 under cyclic loading with intersection of dash lines indicating ‘nominal yield’

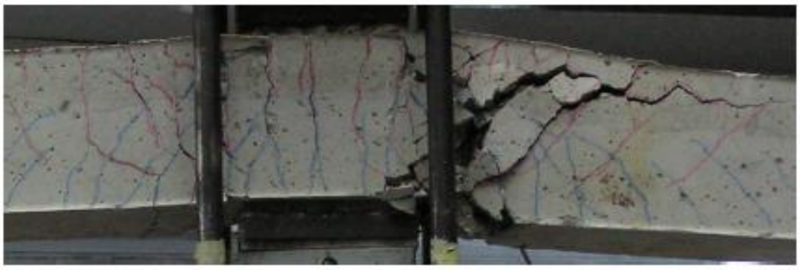

LWAC-S-C2

Fig. 20 Failure mode of beam LWAC-S-C2 under cyclic loading

of LWAC to the column shear capacity.

Figs. 21 and 22 show the variation of the energy dissipated with successive load cycles corresponding to increasing values of the ductility ratio. The figures show that all specimens exhibit similar trends of behaviour. After an initial slow rate of increase, the dissipated energy increases at an increasing rate up to the value of the ductility ratio essentially corresponding to the peak displacement level.

All specimens exhibited similar crack patterns up to the load cycle that preceded loss of load-carrying capacity. Therefore, only the modes of failure of the specimens tested are depicted in Figs. 6, 8, 14, 16, 18, and 20. From the figures, it can be seen that, in contrast with the beams made of NC (beams NC-R-C and NC-S-C), those made of LWAC (beams LWAC-R-C1/2 and LWAC-S-C1/2) fail in flexure in the region of their mid span cross section. On the other hand, failure of the beams made of NC is characterised by extensive inclined criss-crossing cracking in their shear span. The mode of failure exhibited by the specimens appears to be linked with the number of load cycles sustained by the specimens: the appearance of inclined cracking accelerates the cracking processes and leads to loss of load-carrying capacity at an earlier stage of the cyclic loading.

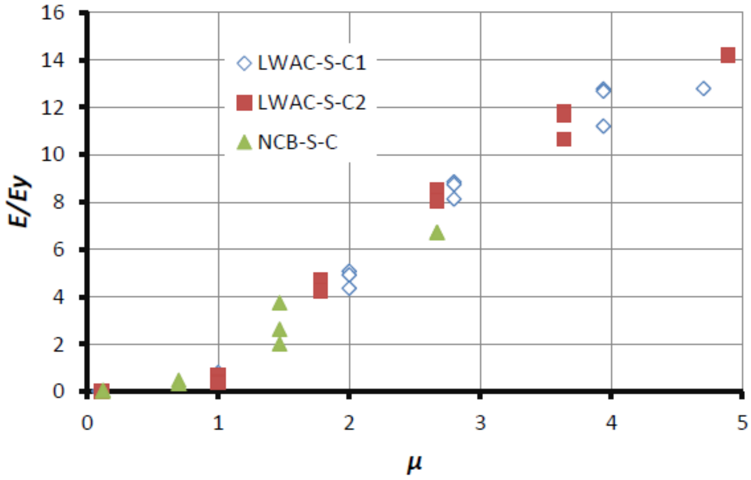

Fig. 21 Energy dissipated during the loading cycles leading to failure of the beams with a square cross section under cyclic loading

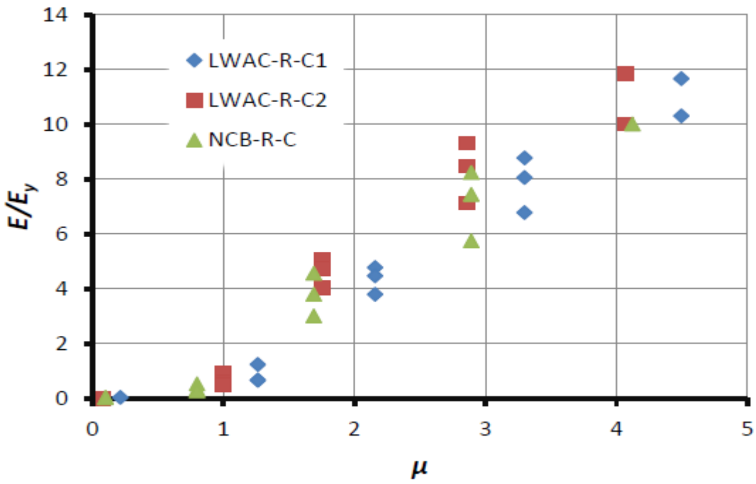

Fig. 22 Energy dissipated during the loading cycles leading to failure of the beams with a rectangular cross section under cyclic loading

From the discussion of the experimental information presented in the paper, it appears that the use of LWAC not only leads to a structural behaviour that satisfies performance requirements of current codes for the design of earthquake-resistant RC structures, but also improves structural behaviour as regards ductility and safeguarding against brittle types of failure. These characteristics, combined with the beneficial effects of the reduction of the inertia forces resulting from the significant reduction of the structure’s deadweight and the more uniform load distribution due to internal force redistribution owing to long-term deformations under service conditions, provide an incentive to direct research efforts into a subject that is likely to prove beneficial to the construction industry.

5. Conclusions

The use of LWAC for the construction of RC structures leads to structural behaviour which is similar with, if not better than, that characterising structures made of NC. The results obtained from tests on RC beams indicate that the beams made of LWAC exhibit a load-carrying capacity similar to that of the RC beams made of NC for the cases of both monotonic and cyclic loading. Although the stiffness of the LWAC beams can be up to about 30% smaller than the stiffness of the NC beams, the use of LWAC is found to lead to a considerable improvement of the post-peak structural behaviour. Combining the above structural characteristics with the reduction of the inertia forces resulting from the significant reduction of the structure's deadweight, the use of LWAC is expected to lead to significant savings without compromising the structural performance code requirements for earthquake resistance RC structures.

References

Ahmad, S.H. and Barker, R. (1991), "Flexural behavior of reinforced high-strength lightweight concrete beams", *ACI Struct. J.*, **88**(1), 69-77.

Ahmad, S.H. and Batts, J. (1991), "Flexural behavior of doubly reinforced high-strength lightweight concrete beams with web reinforcement", *ACI Struct. J.*, **88**(3), 351-358.

American Concrete Institute (1998), *Standard practice for selecting proportions for structural lightweight concrete* (ACI 211.2-98).

American Concrete Institute (2011), *Building code requirements for structural concrete* (ACI 318-11) *and commentary* (ACI 318-11R).

Bertero, B.G., Popov, E.P. and Forzani, B. (1980), "Seismic behavior of lightweight concrete beam-column subassemlages", *ACI Struct. J.*, **77**(1), 44-52.

Campione, G., Cucchiava, C., La Medola, L. and Papia, M. (2005), "Steel-concrete bond in lightweight fiber reinforced concrete under monotonic and cyclic actions", *Eng. Struct.*, **27**(6), 881-890.

Chai, Y.H. and Anderson, J.D. (2005), "Seismic response of perforated lightweight aggregate concrete wall panels for low rise modular classrooms", *Eng. Struct.*, **27**(4), 593-604.

Clarke, J.L. (1993), *Structural Lightweight aggregate concrete*, Blackie Academic & Professional.

Demirboga, R. (2007), "Thermal conductivity and compressive strength of concrete incorporation with mineral admixtures", *Build. Environ.*, **42**, 2467-2471.

Eurocode 2 (EC2) (2004), *Design of concrete structures. Part 1-1: General rules and rules of building*, British Standards.

Eurocode 8 (EC8) (2004), *Design of structures for earthquake resistance. Part 1: General rules, seismic actions and rules for buildings*, British Standards.

Ghosh, S.K., Narielwada, D.P., Shin, S.W. and Moreno, J. (1993), "Flexural behavior including ductility of high strength lightweight concrete members under reversed cyclic loading", *ACI SP136-10*, **136**, 357-376.

Gunduz, L. (2008), "The effects of pumice aggregate/cement ratios on the low-strength concrete properties", *Constr. Build. Mater.*, **22**, 721-728.

Hanson, S.A. (1957), "Shear strength of lightweight reinforced concrete beams", *J. ACI*, **39**(3), 387-403.

Hassan, A. (1999), "Optimising insulation thickness for buildings using life cycle cost", *Appl. Energy*, **63**, 115-124.

Hendrix, S.E. and Kowalsky, M.J. (2010), "Seismic shear behavior of lightweight aggregate concrete square columns", *ACI Struct. J.*, **107**(6), 680-688.

Hognestad, E., Elstner, R.C. and Hanson, S.A. (1964), "Shear strength of reinforced structural lightweight aggregate concrete slabs", *J. ACI*, **61(**6), 643-656.

Ivey, D.L. and Buth, E. (1967), "Shear capacity of lightweight concrete beams", *ACI J.*, **64**(10), 634-643.

Kang, T.H.K., Kim, W., Kwak, Y.K. and Hang, S.G. (2011), “Shear testing of steel fiber-reinforced lightweight concrete beams with web reinforcement ”, *ACI Struct. J.*, **108**(5), 553-561.
Khan, M.I. (2002), “Factors affecting the thermal properties of concrete and applicability of its prediction models”, *Build. Environ*., **37**, 607-614.
Kong, F.K., Teng, S., Sigh, A. and Tan, K.H. (1996), “Effect of embedment length of tension reinforcement on the behavior of lightweight concrete deep beams”, *ACI Struct. J.*, **93**(1), 21-29.
Kotsovos, G.M. (2011), “Seismic design of RC beam-column elements”, *Mag. Concrete Res*., **63**(7), 527-537.
Kotsovos, G.M., Vougioukas, E. and Kotsovos, M.D. (2013), “Reducing steel congestion without violating seismic performance requirements”, *ACI Struct. J.*, **110**(3), 427-436.
Kovalsky, M.J., Priestley, M.J.N. and Seible, F. (1999), “Shear and flexural behaviour of lightweight concrete bridge columns in seismic regions”, *ACI Struct. J.*, **96**(1), 136-148.
Kripanarayanan, K.M. and Branson, D.E. (1972), “Short-time deflections of beams under single and repeated load cycles”, *ACI J.*, **69**(2), 110-117.
Marzouk, H., Osman, M. and Hussein, A. (2001), “Cyclic loading of high-strength lightweight concrete slabs”, *ACI Struct. J.*, **98**(2), 207-214.
Mitchell, D.W. and Marzouk, H. (2007), “Bond characteristics of high-strength lightweight concrete”, *ACI Struct. J.*, **104**(1), 22-29.
Neville, A.M. (1999), *Properties of concrete*, Longman, UK.
Rabbat, B.G., Daniel, J.I., Weinmann, T.L. and Hanson, L.W. (1986), “Seismic behavior of lightweight and normal weight concrete columns”, *ACI J. Proceedings*, **83**(1), 69-79.
Salamandra, M.A. and Ahmad, S.H. (1990), “Shear capacity of reinforced lightweight high-strength concrete beams”, *ACI Struct. J.*, **86**(5), 697-704.
Schaumann, E., Vallee, T. and Keller, T. (2009), “Modelling of direct load transmission in lightweight concrete-core sandwich beams”, *ACI Struct. J.*, **106**(4), 435-444.
Short, A. and Kinniburg, W. (1978), *Lightweight concrete*, *Great Britain*, Galliard (printers) Ltd, Great Yarmouth.
Sim, L.H., Huan, W.T., Islam, M.R. and Mansur, M.A. (2011), “Reinforced lightweight concrete beams in flexure”, *ACI Struct. J.*, **108**(1), 3-10.
Swamy, R.N. and Lambert, G.H. (1984), “Flexural behaviour of reinforced concrete beams made with fly ash coarse aggregates”, *Int. J. Cement Compos. Lightweight Concrete*, **6**(3), 189-200.
Yang, K.H. (2010), “Tests on lightweight concrete deep beams”, *ACI Struct. J.*, 1**07**(6), 663-670.
Yang, K.H., Sim, J.I. and Kang, T.H.K. (2013), “Generalised equivalent stress block model considering varying concrete compressive strength and unit weight”, *ACI Struct. J.*, **110**(5), 791-799.

SA

Notations

b	beam width
d	beam depth
L	beam total length
a_{ss}	shear span
s	span
f_c	uniaxial cylinder compressive strength
f_y	yield stress of steel bar
M_f	flexural capacity of beam

M_y	bending moment of beam corresponding at first yielding (of either concrete or reinforcing steel)
P_e	experimentally-established load-carrying capacity of beam
P_f	load-carrying capacity of beam corresponding to M_f
P_y	load corresponding to M_y
V_f	shear force corresponding to M_f
$\delta_{y,n}$	displacement at nominal yield
δ_{sust}	displacement at last sustained load cycle
δ_{fail}	displacement at final load cycle (failure)
μ_{sust}	ductility ratio corresponding to δ_{sust}
μ_{fail}	ductility ratio corresponding to δ_{fail}